Proceedings of the 2007 IEEE
International Conference on Robotics and Biomimetics
December 15 -18, 2007, Sanya, China

Multisensor Fusion and Navigation for Robot Mower*

Ming Cong and Bo Fang
School of Mechanical Engineering, Dalian University of Technology
Dalian, 116024, China
congm@dlut.edu.cn

Abstract **- This paper presents a multisensor system for combining measurements from ultrasonic sensors and navigation for robot mowers. The proposed sensing system enables robot mowers to mapping unknown environments. It is important for an autonomous robot mower to explore its surroundings in performing the task of localization and navigation for mowing. Because of the complexity of the environment, one simple kind of sensors is not sufficient for robot mower to accomplish these tasks. We develop a robot mower equipped with DSP TMS320F2812 as its CPU. The sensing system integrates with ultrasonic sensors, infrared sensors, collision sensors, encoders, a temperature sensor and an electronic compass. A method of high accuracy ultrasonic ranging technology based on wavelet transform is reported to improve the measurement precision of ultrasonic sensors. Simulation studies show that the proposed multisensor fusion method is very effective for the navigation of robot mowers. Experimental results indicate that this sensing system based on generalized auto-correlation method for obstacle detection and localization shows great potential for providing a high performance-to-price ratio and robust solution for robot mowers in dynamic working condition.**

Index Terms - multisensor fusion, ultrasonic sensors, robot mower, mapping, navigation

I. INTRODUCTION

Lawn mowing is considered by many to be one of the most boring and tiring routine tasks. The environmental robots are needed urgently to perform the task. Some predictions indicate that the robot mowers will be one of the most promising personal robot applications and have substantial market in the world. Therefore, the concept of Intelligent Robot Mower (IRM) had been proposed for the first time in 1997's annual conference of the OPEI (Outdoor Power Equipment Institute) [1]. The robots mainly face to the general families to help the busy people and the hypodynamic old folks save the payments for hiring labours, also remove people from noise, pollen and danger of mowing blade. The robot mowers serve for home care as the outdoor mobile robots, actually kind of intelligent mechatronics devices for environment clean-up [2][3]. The important thing is that the robot mowers are representative of some area-covering environmental robots used not only for indoor floor cleaning as in [4] but also in hazardous environments such as removing landmines, cleaning up radiant points and prospecting for resources etc. The robot mowers get great challenges differing from indoor mobile robots.

The robot mowers use sensors to understand environments as well as their real-time states for obstacle avoidance, map building, location and navigation in the whole work area. Because of the complexity of the environment, one simple kind of sensors is not sufficient for robot mower to accomplish these tasks. It is necessary to combine the observed sensor data coming from different sensors to reduce the uncertainties of the robot in any working environment. To merge the information from the various sensors, robust and real-time sensor fusion is required [5]. In cases of sensor error or failure, multisensor fusion can also reduce uncertainty in the information and increase its reliability.

A sensing system of low cost, low power consumption, high performance is described. The detecting range of ultrasonic sensors is 0.3m~5m, they provide good range information. However, uncertainties in ultrasonic sensors caused by the specular reflection from environments make them less attractive. The detecting range of infrared sensors is 0.02m~1m, they can detect the obstacles within the ultrasonic sensor's blind zone.

In order to satisfy the needs of robot mowers for the low cost and high accuracy ranging technology, the research on the high accuracy ultrasonic ranging technology based on wavelet transform (WT) is reported to improve the measurement precision of ultrasonic sensors. Measurement data gathered from the sensing system are integrated to avoid the robot mower from unknown obstacles and plan an optimum, reliable and realizable plan completely coverage of entire working area.

Finally, simulation studies and experimental results show the effectiveness of the sensing system for the navigation, obstacle detection and localization of robot mowers.

II. SYSTEM HARDWARE OF IRM

The IRM uses DSP TMS320F2812 as its CPU, including four units: vehicle system, cutting system, sensing system and control system. The sensing system is used to collect the external dynamic information of the working environment for obstacle avoidance, map building, navigation and localization. It is also used to detect vehicle system's movement parameters and cutting mechanism's working status. The controller compares the acquired information with the database, and then sends out revisory and accurate command to the robot to perform its tasks. The hardware of the IRM is shown in Fig. 1.

* This work is supported by national natural science fund #50675027to Ming Cong

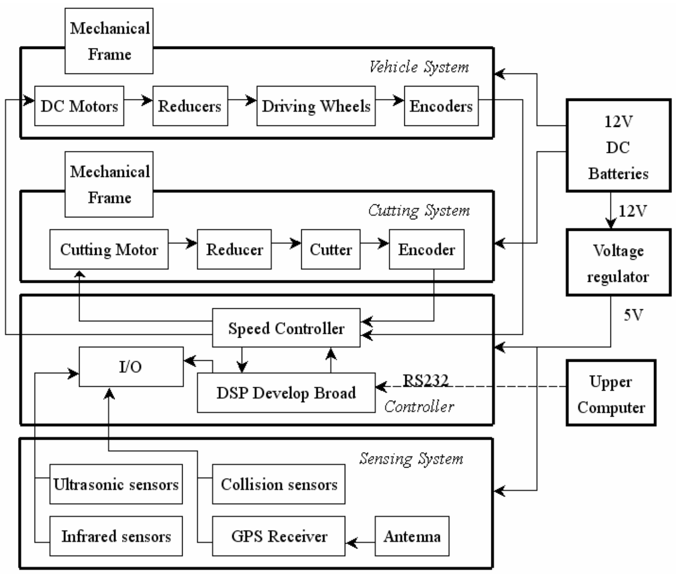

Fig. 1 Hardware overview of IMR

The robot must be physically strong, computationally fast, behaviourally accurate and safety. It should have the ability to perform on its own, and required no human intervention during the whole or most part of the mowing period. The IRM is modularized designed and each unit of the IRM is relatively independent. Modularized design makes the maintenance much easier. Any broken unit of the IRM can be replaced directly without influencing the functions of other units.

III. SENSING SYSTEM

A. Ultrasonic Sensor Unit

Because ultrasonic sensors can provide good range information based on the time of the flight (TOF) principle, mainly due to their simplicity and relatively low cost, they have been widely used in mobile robots for obstacle avoidance, map building and so on. This type of external sensor is very good in obstacles distance measurement. The main lobe of the sensitivity function is contained within an angle of 20 degrees, as shown in Fig. 2 [6]. A number of tests showed that the range accuracy of the sensors is in the order of ±2cm.

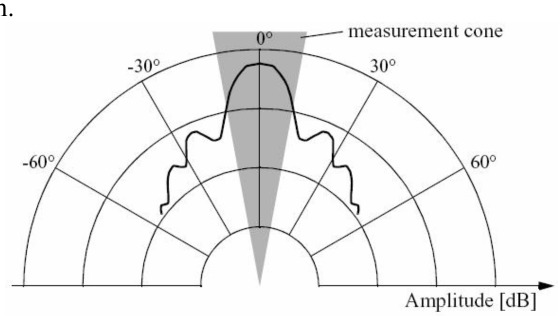

Fig. 2 Typical intensity distribution of an ultrasonic sensor

On IRM, we set up a sensor array which consists of 12 ultrasonic sensors spaced 30 degrees apart. The ultrasonic signals can cover all the space around and satisfy the space requirement about which robot can detect the environmental signals. Classical techniques used in ultrasonic transducers are based on TOF measurement, which calculates the distance of the nearest reflector using the speed of sound in air and the emitted pulse and echo arrival times. The distance d to a reflected object is calculated by

$$d = (c \times t)/2 \tag{1}$$

where c is the speed of sound, and t is the time-of-flight. The TOF method produces a range value when the echo amplitude first exceeds the threshold level after transmitting, ignoring a second echo from a further reflector.

The ultrasonic sensor unit includes a trigger pulse generation unit, a multi-channel selection unit and an echo receiving unit. A sensor interface circuitry designed to send and receive ultrasonic sound pulses catches always the first returning echo. The range data related to an object is considered to be on the conic axes even if it is located off the axes.

The ultrasonic wave typically has a frequency between 40 and 180 kHz, and the frequency of the ultrasonic sensors used in the system is 40 kHz. The beam angle is 20 degrees. The 40 kHz PWM pulse is generated by the general-purpose timer unit of DSP. To drive the transmitter effectively and not to bring much vibration, an 8 cycle burst of ultrasound at 40 kHz is sent out once a time. When the ultrasonic pulse is emitted, the sensor will experience “ringing”. Ringing caused by the transmitted pulse can cause the receiver to detect a false echo. This problem is solved by not enabling the capture interrupt of DSP until a delay interval has passed. This means that the ranger can not detect an object whose distance from the sensor is less than half the distance that sound travels during the delay interval. This is the blind zone of the ultrasonic sensor, as shown in Fig. 3.

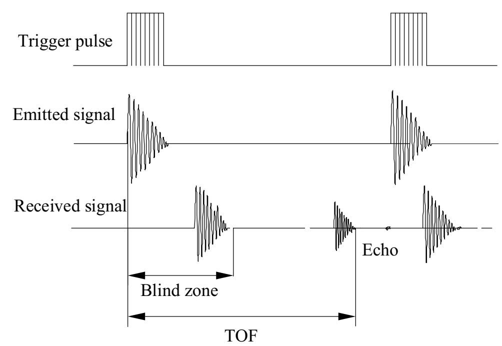

Fig. 3 The sketch map of ultrasonic transmission and reception

B. Infrared Sensor Unit and Other Sensors

To overcome the ultrasonic sensor’s blind zone, infrared sensors are added. The infrared sensors can detect obstacles within 20cm, which patch up the problem caused by the blind zone problem of ultrasonic sensors.

This unit has 16 infrared sensors. Each infrared range finder has a conic view of 6 degrees which is the main lobe of the sensitivity function. This sensor has a useful measuring range of a target up to about one meter with high accuracy. A number of tests showed that the range accuracy of the sensors is in the order of ±lcm.

In order to save the DSP’s resource, 16 infrared sensors are connected with DSP TMS320F2812’s data interface instead of the IO interface. This kind of architecture can also read the sensors' status at the same time, ensuring the real-time capability of the system. A sensor interface circuitry designed to send and receive infrared pulses catches always the first retuning echo to process its amplitude.

Robot mower works in an outdoor environment, where the temperature changes rapidly. The changing of temperature will affect the speed of sound. Therefore, a temperature sensor is used to guarantee the precision of the ultrasonic sensor. Collision sensor is a group of sensitive swatches, which used to prevent the damage caused by unexpected collision. Because moist environment do harm to the circuit of the IRM, humidity sensors are introduced to detect the humidity of the environment. Although these sensors are not absolutely necessary for an autonomous robot mower, they can provide helpful functions to make the work availability and safety.

IV. Sensor-based Navigation

A. Mapping

As seen in Fig. 4, a reference direction x is defined and the robot coordinates are shown as x_R, y_R. By the help of an electronic compass built in on the robot [7], the angle θ_i, which is the *ith* sensor's angle from the 1*st* sensor, can be easily measured. Actually if only the angle θ_S (heading angle of the robot) is measured, other sensor angles can be found as

$$\beta_i = \theta_S + \theta_i \tag{2}$$

where β_i is the angle to the our world coordinate center. The number of maximum sensor group on the ultrasonic ring is *n*, and the radius is *r* (in our system *n*=12 and *r*=0.25m). The distance between the origin and the center of the ring is *R*, and reference angle to the center is Ω. The reference position of the robot's center is (x_R, y_R). The distance from the origin to object which is detected by the *ith* sensor data on the two dimensional plane is called R_i.

Now let dm_i denote measured value which is combined data from the ultrasonic and infrared sensors, for the exact distance R_i. There will be an error δ_i between these values as

$$dm_i = d_i + \delta_i. \tag{3}$$

In this work we naturally assume that δ_i is a uniform random variable in the range of (-*W*, *W*). Here *W* denotes the maximum distance measurement error.

Here the problem is, given x_R, y_R, *r*, $\theta_1, \theta_2, \cdots, \theta_n$, and $dm_1, dm_2, \cdots, dm_n$, to estimate the coordinates of the occupied cells x_i and y_i (or equivalently R_i) in most efficient way.

The equations involving the detected object can be written as

$$R_i^2 = (x_R + (r+d_i)\cos(\beta_i))^2 + (y_R + (r+d_i)\sin(\beta_i))^2 \tag{4}$$

$$R_i^2 = R^2 + (r+d_i)^2 + 2(r+d_i)(x\cos(\beta_i) + y\sin(\beta_i))$$

$$R_i^2 = R^2 + (r+d_i)^2 + 2(r+d_i)\cos(\Omega_R - \beta_i) \tag{5}$$

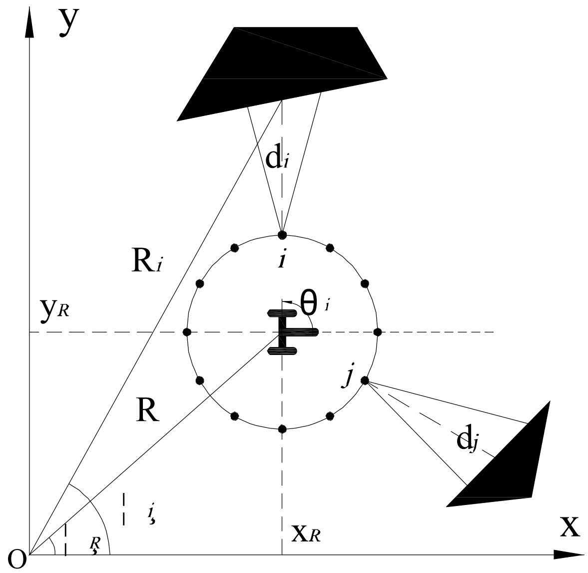

Fig. 4 The robot position on x-y section

The equations involving the robot due to the object can be written as

$$R^2 = (x_i - (r+d_i)\cos(\beta_i))^2 + (y_i - (r+d_i)\sin(\beta_i))^2 \tag{6}$$

$$R^2 = x_i^2 + y_i^2 + (r+d_i)^2 - 2(r+d_i)(x_i\cos(\beta_i) + y_i\sin(\beta_i))$$

If we define the positions as: $P_i = [p_1, p_1 \cdots, p_n]^T = [x_i, y_i]^T$, then we have

$$R^2 = R_i^2 + (r+d_i)^2 - 2(r+d_i)\left[\cos(\beta_i), y_i\sin(\beta_i)\right]P_i \tag{7}$$

After the inserting the $R^2{}_i$ in R^2,

$$\left[(r+d_i) + R\cos(\Omega - \beta_i)\right] = \left[\cos(\beta_i), y_i\sin(\beta_i)\right]P_i \tag{8}$$

Here again we have n such equations. And we write them in matrix form

$$[m] = [A]P_i \tag{9}$$

And if we introduce new matrix as $[L(\beta_i)] = [\cos(\beta_i), \sin(\beta_i)]P_i$ and $[\phi] = [0,0]$, then (10), can be written as

$$\begin{bmatrix} r + dm_1 + R\cos(\Omega_R - \beta_1) \\ \cdot \\ \cdot \\ \cdot \\ r + dm_n + R\cos(\Omega_R - \beta_n) \end{bmatrix} = \begin{bmatrix} L(\beta_1) & \phi & \phi & \cdot & \phi \\ \phi & L(\beta_2) & \phi & \cdot & \phi \\ \phi & \phi & \cdot & \cdot & \cdot \\ \cdot & \cdot & \cdot & \cdot & \phi \\ \phi & \phi & \cdot & \phi & L(\beta_n) \end{bmatrix} \begin{bmatrix} p_1 \\ \cdot \\ \cdot \\ \cdot \\ p_n \end{bmatrix}$$

Here if we perform the least squares estimate for P_i, we obtain

$$(P_{lsq})_i = (A^T A)^{-1} A^T m \tag{11}$$

Thus we find the best squares estimate of the positions.

B. Simulation Studies

Sensor-based navigation has been tested with simulation to shown the usefulness of this sensor fusion method in the two environments respectively as shown in Fig. 5 and Fig. 6. The mower has been primarily tested in a structured laboratory as shown in Fig. 5. Start at (0.3m, 0.5m, 0degree), a virtual robot was driven around a virtual square corridor one time. The walls in the artificial environment are denoted by the real map.

The entire vehicle is self-contained. It has a maximum travel speed on 0.4 m/s. The laboratory area was surveyed out to a 10cm grid with accuracy better than about 1cm. To extract the mapping, a start and goal points were presented. The robot position and orientation were established by the electronic compass [8].

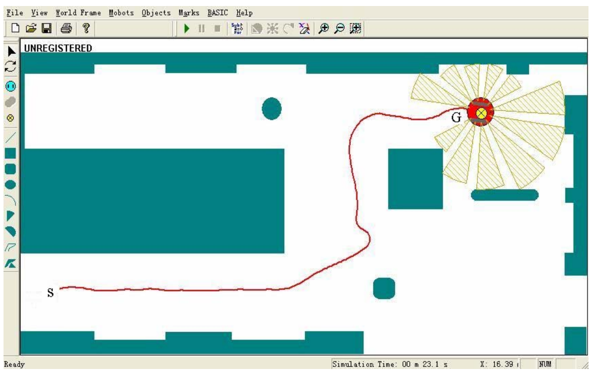

Fig. 5 Data collection and navigation result in structured environment

The result in Fig. 5 demonstrates the mapping quality and the usefulness of this sensor fusion method. In the tests, we find that the average error (ε) in estimating the position of the obstacles in the environment was in the range of [-0.2, 0.2]m.

In the simulations we see that $(P_{lsq})_i$ in (11), obtained does not satisfy $R_i = \|(P_{lsq})_i\|$ which actually should. In the case a better estimate for the positions can be given as

$$(P_e)_i = (P_{lsq})_i \frac{\|R_i\|}{\|(P_{lsq})_i\|} \tag{12}$$

In this case, estimate for the angle Ω_i does not change but the estimate for distance R_i is scaled to it best estimate. Therefore for the position, the distance estimate R_i remains the same as before, while the least squares estimate works only for the angle Ω_i . Simulations show that this way produces more accurate results.

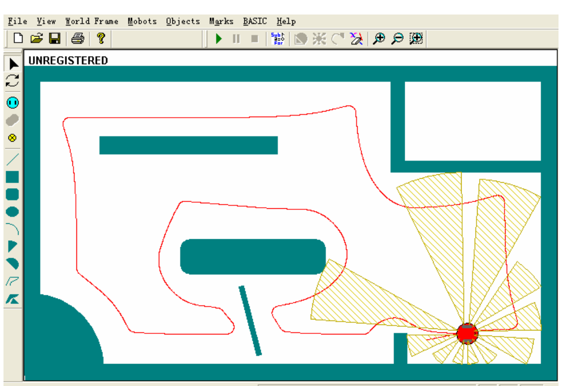

Fig. 6 The simulation result of wall-following behavior

Wall following was selected for the initial problem domain because it is a fairly simple problem to set up and evaluate [9]. It also lays the groundwork for more complex problem domains, such as maze traversal, mapping and complete coverage path planning which is used on lawn mowing and vacuuming. The simulation result of wall-following behavior shown in Fig. 6, and the experimental result in Fig. 6 demonstrate that the IRM have the capability to perform its mowing task in unstructured environment.

The program of sensor-based navigation simulation in Fig. 5 is given below.

```
Sub Main
        Dim PI,Fcr,Fct,X_target,Y_target,X,Y As Single
        Dim X_grid, Y_grid, i, j, C As Integer
        Dim Frx,Fry,d, dist_targ, rot, Fx, Fy As Single
        Dim Fcx,Fcy, Rx,Ry As Single
        PI=3.1415927
        Fcr=1
        Fct=1
        X_target=GetMarkX(0)
        Y_target=GetMarkY(0)
        SetCellSize(0,0.1)              'Set cell size 10 cm x 10 cm
        SetTimeStep(0.1)     'Set simulation time step of 0.1 seconds

    Do                                   ' Start main loop
         X=GetMobotX(0)    'Present mobot coordinates (in meters)
         Y=GetMobotY(0)
         X_grid=CoordToGrid(0,X)       ' indexes of cells where the
         Y_grid=CoordToGrid(0,Y)            ' mobot center is
         MeasureRange(0,-1,3)  ' Perform a range scan and update
                          ' the Certainty Grid (max. cell value=3)
         Frx=0
         Fry=0
            ' Each ocuppied cell inside the windows of 33 x 33 cells
                ' applies a repulsive force to the mobot.

    For  i=X_grid-16 To X_grid+16
              For j=Y_grid-16 To Y_grid+16
                   C=GetCell(0,i,j)
                     If C>0 Then
                        d=Sqr((X_grid-i)^2+(Y_grid-j)^2)
                          If d>0 Then
                            Frx=Frx+Fcr*C/d^2*(X_grid-i)/d
                            Fry=Fry+Fcr*C/d^2*(Y_grid-j)/d
                        End If
                   End If
              Next
         Next
     dist_targ=Sqr((X-X_target)^2+(Y-Y_target)^2)
         Fcx=Fct*(X_target-X)/dist_targ
         Fcy=Fct*(Y_target-Y)/dist_targ
         Rx=Frx+Fcx
         Ry=Fry+Fcy
         rot=RotationalDiff(0,X+Rx,Y+Ry)
                          'shortest rotational difference between
              'current direction of travel and direction of vector R
         SetSteering(0,0.5,3*rot)'mobot turns into the direction of R
                           'at constant speed and steering rate
                        'proportional to the rotational difference
         StepForward
    Loop Until dist_targ<0.1   'Loop until mobot reaches the target
End Sub
```

V. ULTRASONIC RANGING TECHNOLOGY BASED ON WT

Unfortunately, the practical received multi-echoes has time-varying property and is a typical non-stationary signal because the influence of the environmental complexity and the noise. Furthermore, the noise mixed in the ultrasonic pulse-echo is Non-Gaussian white noise but colored noise, and correlated with the target echo. The TOF method can not be used directly in such conditions. Referencing the generalized correlation method for estimation of time delay [10], we put forward the generalized auto-correlation method for estimation of time-of-flight based on wavelet transform [11] and present in Fig. 7.

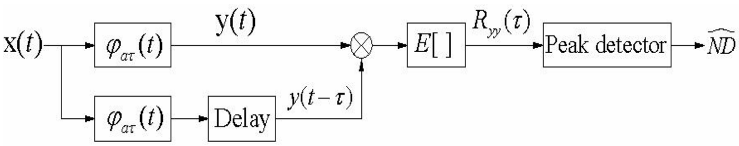

Fig. 7 Delay estimation of generalized auto-correlation based on WT

Where $\varphi(t)$ is the mother wavelet and $\varphi_{\alpha\tau}(t)$ is the daughter wavelet. The coefficient α is the scale (or scaling factor) and τ is the time displacement. The wavelet transform of the signal $x(t)$ is $y(t)$. Actually this is a filtering process of the ultrasonic echo using a multitude of bandpass filters of equal Q, which is equivalent to the whitening filter of the generalized correlation method for estimation of time delay, in order to eliminate the input noise which can influence the following processing. $R_{yy}(\tau)$ can be found as

$$R_{yy}(\tau) = E[y(t)y(t-\tau)] = R_{xx}(t) * [\varphi_{\alpha\tau}(t) * \varphi_{\alpha\tau}(-t)]$$

As there has the relationship of Fourier transform between auto-correlation function $R_{yy}(\tau)$ and his power spectrume:

$$G_{yy}(\omega) = F[R_{yy}(\tau)] = G_{xx}(\omega)\Psi(a\omega)\Psi^*(a\omega) = G_{xx}(\omega)\left|\Psi(a\omega)\right|^2$$

We obtain the generalized auto-correlation function as

$$R_{yy}^{(g)}(\tau) = \frac{1}{2\pi}\int_{-\infty}^{\infty} G_{yy}(\omega)e^{j\omega\tau}d\omega = \frac{1}{2\pi}\int_{-\infty}^{\infty} \psi_g(\omega)G_{yy}(\omega)e^{j\omega\tau}d\omega$$

Last, the peak values of $R_{yy}(\tau)$ are detected to accomplish the estimation of TOF and calculate the real ultrasonic velocity.

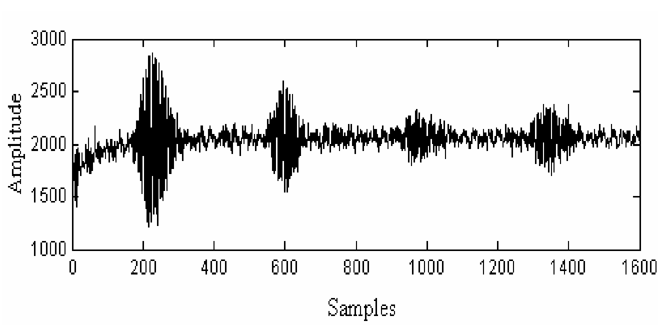

Fig. 8 Noisy ultrasonic echo

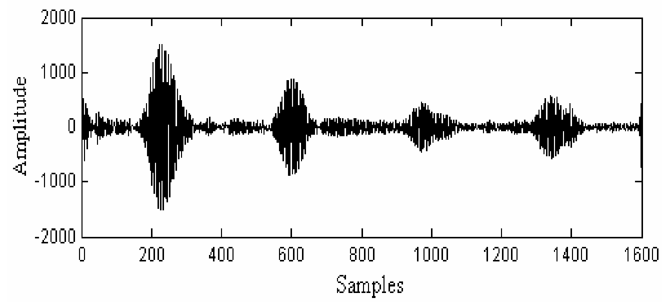

Fig. 9 Denoised echo using WT

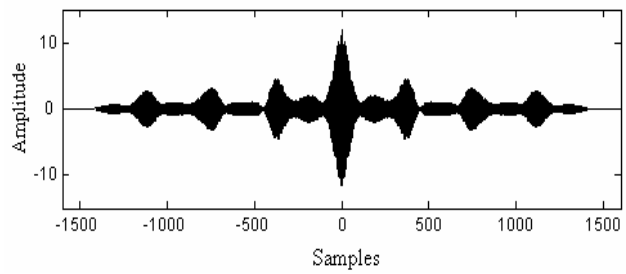

Fig. 10 Auto-correlation function $R_{yy}(\tau)$

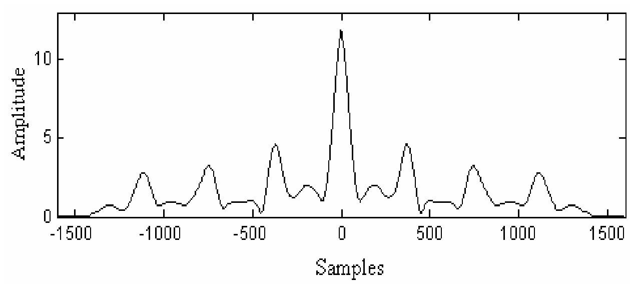

Fig. 11 Peak detection

The noisy ultrasonic echo is shown in Fig. 8, and the denoised ultrasonic echo by wavelet transform is shown in Fig. 9. It is obvious that the noise mixed in the ultrasonic echo is effectively eliminated after WT operation. The auto-correlation operation $R_{yy}(\tau)$ of the denoised ultrasonic echo is shown in Fig. 10. Fig. 11 shows the envelope of $R_{yy}(\tau)$ through Hilbert transform. As we can see, if the abscissa of every peak point is determined, the estimation of TOF $\widehat{ND}$ can be calculated. Considered the attenuation of the ultrasonic echo and the demand of the high precision in practice, only the former four echoes are used to estimate the TOF. The values of the TOF estimation are $\widehat{-3D}, \widehat{-2D}, \widehat{-D}, \widehat{D}, \widehat{2D}, \widehat{3D}$, which are symmetrical to the x-axis. Using this method, the estimation of the ultrasonic velocity can be calculated.

So far, an obstacle detection and localization system has been implemented successfully. By means of above method, an obstacle detection and localization system has been implemented successfully.

The generalized auto-correlation method based on wavelet transform is put forward to realize the real-time ultrasonic velocity measurement, and this method can eliminate the influence of temperature, humidity and wind on ultrasonic velocity measurements when the robots are working in dynamic condition. And this sensing system based on generalized auto-correlation method shows great potential for providing a robust solution for robot mowers in dynamic working condition.

VI. Experimental Results

We measure the distance between the robot and plane objects using the ultrasonic sensors. The measured results and the actual distances are shown in TABLE I.

TABLE I
THE EXPERIMENTAL DATA OF THE ULTRASONIC SENSORS (unit: cm)

Actual distance	Measured value1	Measured value2	Average error
30	30.62	30.61	2.50%
40	40.70	41.69	1.73%
50	50.64	50.67	1.31%
60	60.73	60.73	1.22%
70	70.81	70.84	1.19%
80	81.09	81.04	1.33%
90	91.10	91.13	1.24%
100	98.82	99.15	1.02%
150	148.24	148.37	1.13%
200	201.85	201.85	0.93%
250	252.71	252.74	1.09%
300	302.52	302.58	0.85%
350	347.63	347.61	0.68%
400	405.75	405.77	1.44%
450	456.22	456.26	1.39%
500	508.87	508.90	1.77%

From TABLE I, we can see that the measurement error of the ultrasonic sensor is within 3%.

Then, the generalized auto-correlation method based on wavelet transform is put forward to realize the real-time ultrasonic velocity measurement.

By means of above method, we measure the distance between the robot and plane objects again. The measured results and the actual distances are shown in TABLE II.

TABLE II
THE DATA BASED ON WAVELET TRANSFORM OF ULTRASONIC SENSORS (unit: cm)

Actual distance	Measured value1	Measured value2	Average error
30	30.23	30.22	0.75%
40	40.27	40.25	0.65%
50	50.28	50.28	0.56%
60	60.24	60.27	0.43%
70	70.32	70.31	0.45%
80	80.40	80.44	0.53%
90	90.43	90.43	0.47%
100	100.49	100.52	0.51%
150	150.58	150.55	0.38%
200	200.71	200.76	0.37%
250	250.68	250.71	0.28%
300	300.75	300.79	0.26%
350	350.83	350.84	0.24%
400	400.96	401.03	0.25%
450	451.32	451.28	0.29%
500	502.52	502.49	0.50%

The experimental results based on wavelet transform indicate that the errors of measurements using above technology are less than 1% within the ranging area of 5m, and this sensing system for obstacle detection and localization shows great potential for providing a high performance-to-price ratio and robust solution for robot mowers in dynamic working condition.

VII. Conclusion

In this paper, we have presented a multisensor system for combining measurements from ultrasonic sensors and navigation for robot mowers. The proposed sensing system has the advantages of low cost, low power consumption, high performance and enables robot mowers to mapping unknown environments. The effectiveness is demonstrated through the simulation studies and experimental results.

Using different kinds of sensors integrated in the sensing system can overcome the ultrasonic sensor's drawbacks of the blind zone and the specular reflection by multisensor fusion.

A method of high accuracy ultrasonic ranging technology based on wavelet transform has been introduced to improve the measurement precision of ultrasonic sensor for more accurate sensory information. This system is applied in the robot mower and proves reliable and real-time in experiments.

Future work will aim at applying the proposed tracking technique to the multisensor fusion scheme is applied to the control of the robot mower in unstructured environments and complete coverage path planning [12].

References

[1] Rob. Warren Hicks and Ernest L. Hall, "A Survey of Robot Lawn Mower," *Intelligent Robots and Computer Vision*, pp. 262-269, 2000.

[2] Li Zu, Huakun Wang and Feng Yue, "Localization for Robot Mowers Covering Unmarked Operational Area," *Proc. of the IEEE International Conf. on Intelligent Robots and Systems*, pp.2197-2202, 2004.

[3] Huakun Wang, Li Zu and Feng Yue, "Neural Networks-Based Terrain Acquisition of Unmarked Area for Robot Mowers," *IEEE International Conf. on Control, Automation, Robotics and Vision*, pp.735-740, 2004.

[4] Chaomin Luo, Simon X. Yang and Max Meng, "Entire region filling in indoor environments using neural networks," *Proc. of the 4th World Congress in Intelligent Control and Automation*, pp. 2039-2044, 2002.

[5] Ofir Cohen and Yael Edan, "A Sensor Fusion Framework for On-Line Sensor and Algorithm Selection," *Proc. of the IEEE International Conf. on Robotics and Automation*, pp. 3155-3160, 2005.

[6] Roland Siegwart and Illah R. Nourbakhsh, *Introduction to Autonomous Mobile Robots*, Cambridge, London: The MTT Press, 2004.

[7] Tun Yang, Member, IEEE and Victor Aitken, "Evidential Mapping for Mobile Robots With Range Sensors," *IEEE Trans. on Instrumentation and Measurement*, vol. 55, no. 4, pp.1422-1429, 2006.

[8] L. Yenilmez and H. Temeltas, "Enabling an autonomous mobile robot to determine its actual position and orientation by using an ultrasonic ring," *4th International Conf. on Automation, Robotics and Vision,* pp. 1125-1129, 1996.

[9] Eduardo Zalama, Jaime Gómez, Mariano Paul, and José Ramón Perán "Adaptive Behavior Navigation of a Mobile Robot," *IEEE Trans. on systems, man and cybernetics-part A: systems and humans*, vol.32, 160-169, 2002

[10] C. Knapp, G. Carter. "The Generalized Correlation Method for Estimation of Time Delay," *IEEE Trans.* on Acoustics, Speech, and Signal Processing, vol24, pp.320-327, 1976.

[11] N. Michalodimitrakis and Th. Laopoulos, "On the Use of Wavelet Transform in Ultrasonic Measurement Systems," *IEEE Instrumentation and Measurement Technology Conference*, pp. 589-594, 2001.

[12] Simon X. Yang and Chaomin Luo, "A Neural Network Approach to Complete Coverage Path Planning," *IEEE Trans. on Systems, Man and Cybernetics-part B:* vol. 34, no.1, pp. 249-265, 2004.